AN ADVANCED CONSTITUTIVE MODEL FOR AGF DESIGN: FROM CALIBRATION TO APPLICATION

*U. Schindler [1]
PhD candidate
*(*Corresponding author: u.schindler@tum.de)*

S. Chrisopoulos [1]
Post-doc

R. Cudmani [1]
Full Professor
[1] *Center for Geotechnics, Technical University of Munich*
Munich, Germany

ABSTRACT

The significance of ground freezing is becoming ever more germane, because the design of new urban tunnel systems requires more complex geometries and higher strength of the improved subsoil, which are limited with conventional construction methods. Therefore, advanced constitutive models for frozen soils need to be developed and implemented in finite element analysis (FEA) codes for ground freezing designs under such complex conditions. This study presents a recently proposed elastic-viscoplastic model describing the rate-, stress-, and temperature-dependent mechanical behaviour of frozen granular soils under compressive and tensile loading along with its implementation in a FEA code. After calibrating and validating the model for frozen Manchester fine sand based on single-element tests, we demonstrate the geotechnical and practical advantages of the model by simulating a tunnel excavation supported by a frozen soil body and compare the numerical results with experimental data from the literature. The good agreement highlights the model's ability to predict the stability and evaluate the deformations of frozen soils in AGF scenarios.

KEYWORDS

Constitutive modelling, frozen soils, shear strength, creep, model tests

INTRODUCTION

The construction of new urban tunnelling systems under complex as well as partially unknown geological and hydrogeological boundary conditions and the resulting high damage risk often requires the use of sophisticated subsoil improvement, water tightening and dewatering techniques. Artificial ground freezing (AGF) is an advanced and environmentally friendly construction technique, which temporarily increases the stiffness and strength of the subsoil as well as provides water tightness. Thus, AGF is often preferable to other soil improvement techniques, although the associated construction costs remain a limiting factor. In fact, AGF is still considered an expensive technique compared to conventional construction methods. For instance, existing (semi-)analytical and elastic approaches to the ultimate-limit state and service-limit state analysis of complex AGF applications are often limited and involve relatively thick frozen soil bodies and high safety factors. Consequently, the use of conventional approaches often results in economically unbalanced, over-engineered AGF designs, which is detrimental to the dissemination of sustainable AGF applications. To overcome this limitation, advanced constitutive models for frozen soils offer a unique opportunity for efficient optimisation of the AGF design. These models need to be implemented in finite element analysis (FEA) codes, extensively tested, and validated for AGF scenarios. The constitutive model proposed by Cudmani et al. (2022) and extended by Schindler et al. (2023b) intends to fill this gap and is designated by the acronym EVPFROZEN. This study aims to familiarise researchers and engineers involved in AGF measures with the use of advanced constitutive models, in particular EVPFROZEN. First, we present the basic equations of EVPFROZEN and explain the user-friendly

EVPFROZEN calibration procedure. We then test the model in small- and large-scale freezing tests and compare the model response with data from the literature. Based on this comparison, we derive the advantages of using the sophisticated constitutive model EVPFROZEN for future AGF designs.

BASIC EQUATIONS OF EVPFROZEN

The main constitutive equations of the proposed elastic-viscoplastic model for frozen granular soils are explained below. Further details can be found in Cudmani et al. (2022) and Schindler et al. (2023b).

$$\dot{\boldsymbol{\sigma}} = \mathbf{L} : (\dot{\boldsymbol{\varepsilon}} - \dot{\boldsymbol{\varepsilon}}_{\mathbf{v}}) \tag{1}$$

$\dot{\boldsymbol{\sigma}}$ is the stress rate tensor, $\dot{\boldsymbol{\varepsilon}}$ is the total strain rate tensor, $\dot{\boldsymbol{\varepsilon}}_{\mathbf{v}}$ is the viscous strain rate tensor and $\mathbf{L}$ is the fourth-order isotropic elastic stiffness tensor.

$$\dot{\boldsymbol{\varepsilon}}_{\mathbf{v}} = \|\dot{\boldsymbol{\varepsilon}}_{\mathbf{m}}\| \exp(-\beta) \exp\left(\beta \frac{t^*}{t_m}\right) \left(\frac{t^*}{t_m}\right)^{-\beta} \frac{\mathbf{s}}{\|\mathbf{s}\|} \tag{2}$$

$\mathbf{s}$ is the deviatoric stress tensor, $\|\dot{\boldsymbol{\varepsilon}}_{\mathbf{m}}\|$ is the minimum creep rate, β is a dimensionless material constant and t^* represent the transformed creep time. The transformed creep time t^* has been introduced in the above equation to consider the influence of the loading history on the creep behaviour. It is calculated iteratively via a time integration scheme, which is presented in detail by Schindler et al. (2023b) and, therefore, will not be repeated here.

$$\|\dot{\boldsymbol{\varepsilon}}_{\mathbf{m}}\| = \sqrt{\frac{3}{2}}\dot{\varepsilon}_\alpha \exp\left[\left(\frac{K_1}{\theta+273.4} + \ln \dot{\varepsilon}_\alpha\right)\left(\frac{\sigma_{cr}(p,q,\varphi)}{\sigma_\alpha(\theta)} - 1\right)\right] \tag{3}$$

θ represents the temperature in Celsius, K_1 is a material constant, $\dot{\varepsilon}_\alpha$ is a reference strain rate ($\dot{\varepsilon}_\alpha$ = 1%/min), while the temperature-dependent unconfined stress σ_α at the reference strain rate, the lifetime t_m and the equivalent unconfined creep strength σ_{cr} are defined in equations 4, 5, and 6, respectively:

$$\sigma_\alpha(\theta) = \alpha_1(-\theta)^{\alpha_2} \tag{4}$$

$$t_m = \sqrt{\frac{3}{2}}\, c/\|\dot{\boldsymbol{\varepsilon}}_{\mathbf{m}}\| \tag{5}$$

$$\sigma_{cr}(p,q,\varphi) = \frac{1}{2}\left\{[(B\cos(\varphi - \pi/3) + C)q + Dp] + \sqrt{\left[\left(B\cos\left(\varphi - \frac{\pi}{3}\right) + C\right)q + Dp\right]^2 + 4Aq^2}\right\} \tag{6}$$

The parameters α_1, α_2 and c in equations 4 and 5 are material constants of the 1D-model. In Equation 6, the parameters A, B, C, and D represent material constants of the 3D-model, while p and q denote the Roscoe stress invariants, and φ denotes the Lode angle.

MODEL CALIBRATION FOR FROZEN MANCHESTER FINE SAND

In total, EVFPROZEN consists of eleven parameters, which can be calibrated by using eight standard laboratory freezing tests consisting of 1D and 3D compression and/or creep tests as well as a 1D tensile test. The derivation and determination of the parameters are explained in detail in Cudmani et al. (2022). In the following, we will exemplary determine all eleven parameters for frozen Manchester fine sand (MFS) to illustrate the unambiguous and rather simple model calibration procedure.

According to Martin et al. (1981) and Andersen (1991), Manchester fine sand (MFS) is a uniform quartz and feldspar fine sand obtained from the banks of the Merrimack River (New Hampshire, USA). The mechanical behaviour of frozen MFS has been extensively investigated by Martin et al. (1981), Ting (1981), Andersen (1991) and Swan (1994). Hence, sufficient experimental data is available to fully calibrate EVPFROZEN for frozen MFS. For instance, Martin et al. (1981) and Ting (1981) extensively investigated the uniaxial creep strength of MFS at various temperatures and uniaxial creep stresses. Table 1 summarises the 1D creep tests used to determine the seven 1D EVPFROZEN model parameters.

Table 1. 1D creep tests on frozen MFS ($\rho_d \approx 1.54$ g/cm^3, $S_r \approx 1.0$) after Martin et al. (1981)

Sample no.	θ [°C]	σ_1 [MPa]	$\dot{\varepsilon}_m$ [%/min]	t_m [min]
S8-59	-12.5	9.1	1.69E-02	120
S8-46	-12.5	7.9	2.40E-03	970
S9-1	-18.5	10.6	4.12E-03	465
S8-76	-18.7	8.8	5.46E-04	3200
S9-137	-27.4	10.6	1.26E-04	10,000
S9-134	-27.6	16.5	1.53E-02	165

Following the procedure by Cudmani et al. (2022), the 1D creep test data in Table 1 are evaluated in Figure 1 to determine the 1D parameters c, α_1, α_2, β, and K_1. The corresponding fitting equations and determined parameter values are also shown in the figure.

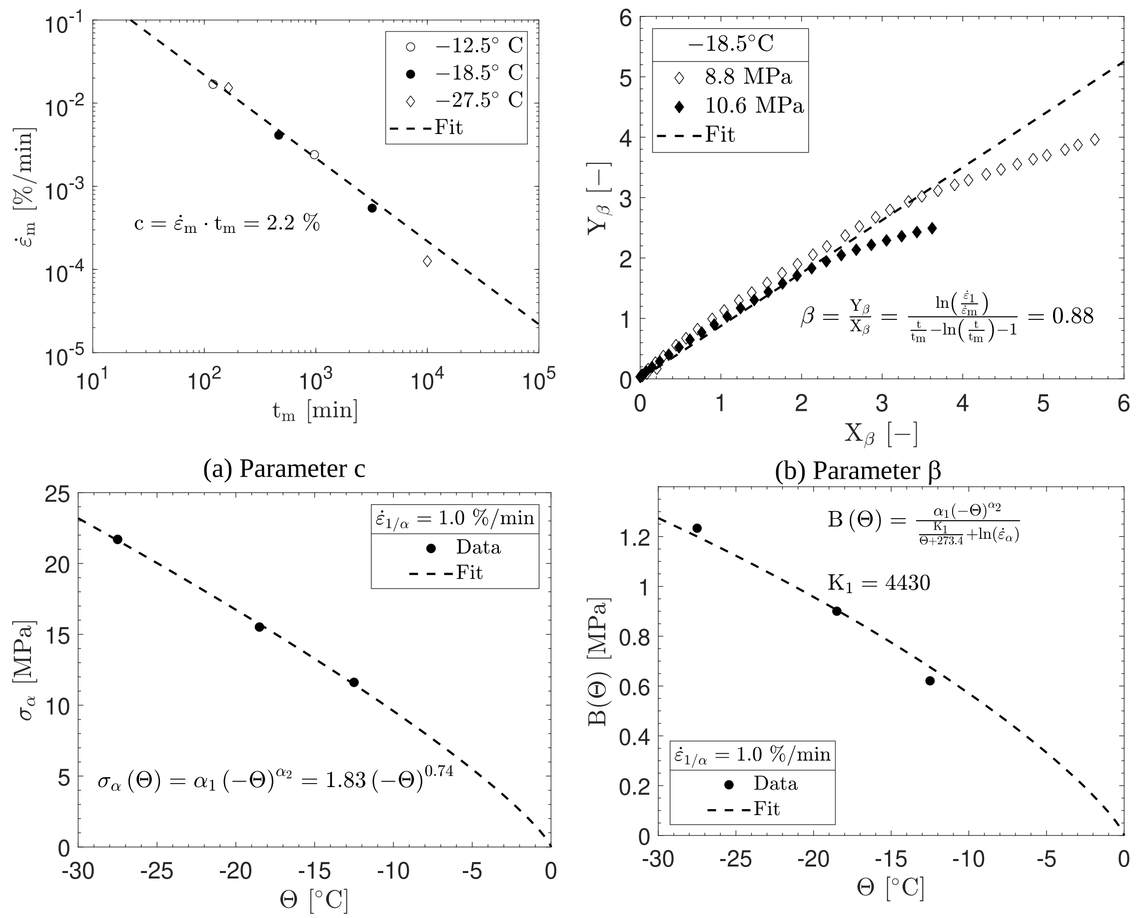

(a) Parameter c (b) Parameter β

(c) Parameter α_1 and α_2 (d) Parameter K_1

Figure 1. Calibration of the 1D model parameters c, α_1, α_2, β, and K_1 using 1D creep tests listed in Table 1. [Data after Martin et al. (1981) and Ting (1981)].

Despite the comprehensive experimental MFS database for compressive loading, there are no sophisticated 1D compression tests with frozen MFS in the literature. Therefore, the Young's modulus E cannot be directly determined. For simplicity, E is assumed to be 500 MPa, which has been approximated from a similar frozen sand found in the literature (Cudmani et al., 2022). According to Martin et al. (1981), the frozen MFS samples tested were fully saturated ($S_r \approx 1.0$). Consequently, the Poisson ratio ν for MFS is assumed to be 0.49.

After calibrating all seven 1D parameters, the missing four 3D parameters A, B, C and D need to be determined to complete the EVPFROZEN calibration procedure. In this context, Andersen (1991) performed comprehensive 3D compression tests on frozen MFS under different constant strain rates and confinements. Table 2 summarises the 3D compression tests used to determine the four 3D model parameters.

Table 2. 3D compression tests on frozen MFS ($\rho_d \approx 1.54\ \mathrm{g/cm^3}$, $S_r \approx 1.0$) at -10°C after Andersen (1991)

Sample no.	σ_3 = const. [MPa]	$\dot{\varepsilon}_1$ [%/min]	q_u [MPa]
18			13.4
19	10	0.180	13.1
63			14.4

As described by Cudmani et al. (2022), EVPFROZEN is capable to account for the influence of the mean pressure and to differentiate between compressive and tensile loading by introducing the equivalent uniaxial creep strength $\sigma_{cr}(p, q, \varphi)$ (see Equation 6). In order to determine the shape of this function, the parameters A, B, C, D are fitted to the results of confined compression tests normalised by their equivalent uniaxial compressive strength (calculated with the 1D model), i.e. $\hat{p} = p/\sigma_{cr}(\dot{\varepsilon}_m, \theta)$ and $\hat{q} = q/\sigma_{cr}(\dot{\varepsilon}_m, \theta)$. Since no tensile tests are available for frozen MFS, we assume empirical points for the hydrostatic tensile strength (0.4, 0) and the ratio of tensile to compressive strength $\sigma_t/\sigma_c = 0.4$, according to data in the literature (Cudmani et al., 2022). In Figure 2, the 3D compression tests from Table 2 are plotted in the normalised $\hat{p} - \hat{q}$ creep surface to determine the 3D parameters A, B, C, D. Again, the corresponding compressive fit equation and the determined parameter values are also shown in the figure. Note that in Figure 2, $\hat{p}$<0 corresponds to compression. Further details of the 3D parameter determination procedure can be found in Cudmani et al. (2022).

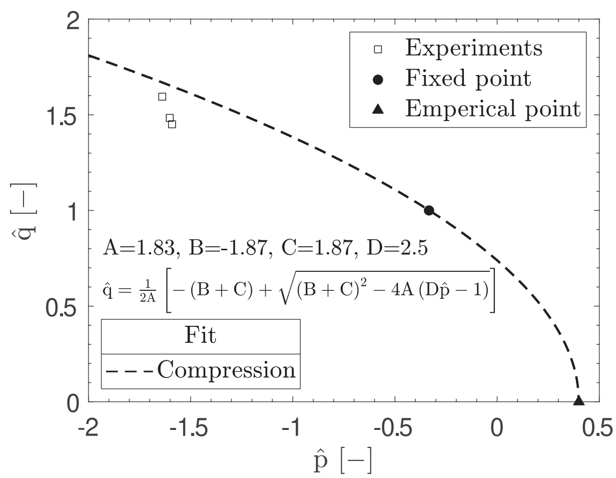

Figure 2. Calibration of 3D EVPFROZEN parameters using 3D compression tests listed in Table 2. [Data after Andersen (1991)].

Table 3 summarises the 1D and 3D material parameters for frozen, saturated MFS with a dry unit weight of $\rho_d \approx 1.54\ \mathrm{g/cm^3}$.

Table 3. EVPFROZEN material constants for frozen Manchester fine sand

1D model							3D model			
E	ν	c	α_1	α_2	β	K_1	A	B	C	D
[MPa]	[-]	[%]	[MPa/°C]	[-]	[-]	[K]	[-]	[-]	[-]	[-]
500	0.49	2.2	1.83	0.74	0.88	4430	1.83	-1.87	1.87	2.5

This is a post-print of the paper accepted for publication at the 11th International Symposium on Ground Freezing (2023), London (UK).
The final version of the paper, including conference editing/formatting, has been published in the corresponding proceedings:
Schindler, U., Chrisopoulos, S., Cudmani, R. 2023. An advanced constitutive model for AGF design: From calibration to application. In 11th International Symposium on Ground Freezing. pp. 517-525. London, UK.

MODEL VALIDATION FOR MFS BASED ON ELEMENT TESTS

This section compares the EVPFROZEN model prediction with the experimental data from uniaxial creep and triaxial compression tests for frozen MFS. Here, Martin et al. (1981) conducted unconfined creep tests at various uniaxial stresses σ_1 and temperatures θ. Figure 3 compares the experimental and numerical results.

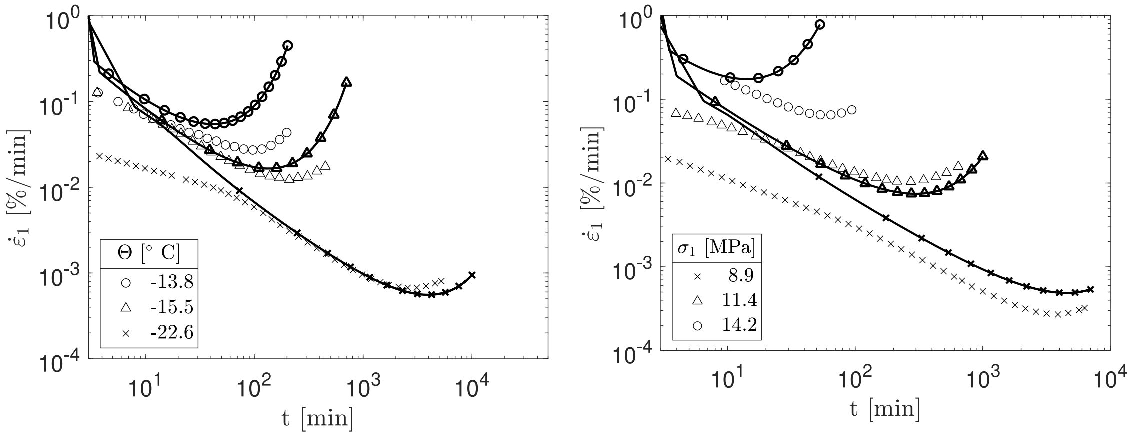

(a) σ_1 = 10.6 MPa (b) θ = -18.4°C

Figure 3. Experimental (symbols) and numerical (lines with symbols) comparison of 1D creep tests with frozen MFS. [Data after Ting (1981)].

The experimental data (open symbols) in Figure 3 show the typical creep behaviour of frozen soils (e.g., Orth, 1986): The axial strain rate first decreased (primary creep) and subsequently increased (tertiary creep) with time. The testing time at which the minimum strain rate $\dot{\varepsilon}_m$ (secondary creep) is reached and the tertiary creep begins is called lifetime t_m according to Orth (1986) and Cudmani et al. (2022). The model response (lines) for the creep tests was in accordance with the experiments. Both the minimum strain rate $\dot{\varepsilon}_m$ and the lifetime t_m were well reproduced, both for different temperatures at a constant uniaxial stress (Figure 3(a)) and for different uniaxial stresses at a constant temperature (Figure 3(b)).

In addition to creep behaviour, EVPFROZEN is also capable of predicting the practically important shear strength of frozen soils under both uniaxial and triaxial loading. Figure 4 compares the experimental and numerical results of triaxial compression tests under different confinements and axial strain rates at -20°C.

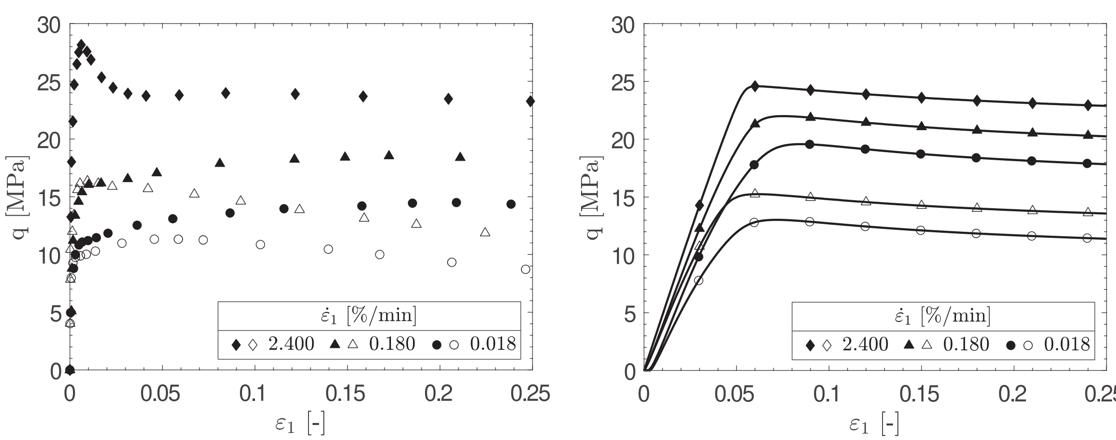

(a) Experiments (a) Simulations

Figure 4. Experimental and numerical comparison of 3D compression tests with frozen MFS tests at -20°C. Filled symbols: σ_3 = 10 MPa; Open symbols: σ_3 = 0.1 MPa. [Data after Swan (1994)].

As can be seen in Figure 4a), the ultimate shear strength q_u of frozen MFS increased with increasing strain rate. In addition, an increase in confinement leads to a higher q_u for the same strain rate $\dot{\varepsilon}_1$. In both cases EVPFROZEN is able to predict the ultimate shear strength accurately (see Figure 4b)). However, the model shows a softer behaviour of the frozen soil before reaching the peak compared to what was measured in the tests. Considering these deviations for MFS, it is recommended that they be taken into account when using the model to evaluate the ultimate-limit state. To sum up, as shown for frozen MFS based on element tests, EVPFROZEN satisfactorily captures the essential characteristics of the shear and creep behaviour of frozen soils, which is key to its use in AGF designs.

SIMULATION OF A TUNNEL EXCAVATION MODEL TEST

In general

Despite the extensive EVPFROZEN testing using single-element tests, advanced constitutive models also need to be tested in boundary value problems approximating practical geotechnical and tunnelling scenarios. In fact, boundary value problems can present much more complex boundary conditions, inducing spatially and temporarily varying stresses, strains, and temperatures, for which the model validation using only single-element tests is limited. This section highlights recent important findings by Schindler et al. (2023a) using EVPFROZEN in simulating a conventional tunnel excavation covered by a frozen soil ring for the excavation step and the following creep step. The full case study can be found in Schindler et al. (2023a).

Description of the test setup and the FEA model

Orth and Meissner (1985) experimentally investigated the creep behaviour of frozen soils using a prototype tunnel at a 1:20 scale. First, the box was filled with dry Karlsruhe medium sand. The filled material was then saturated, and a surface pressure was applied on the top. Subsequently, a frozen horizontal soil cylinder started to form with the help of freezing pipes driven into the sand. The formed frozen soil body enclosed the tunnel excavation area. Finally, the tunnel was excavated with a drilling machine. Displacement transducers and dial gauges monitored the displacements above the tunnel roof at various levels throughout testing. Further description of the model tunnel test can be found in Orth and Meissner (1985). In order to simulate the above-described tunnel excavation problem, a 3D boundary value problem has been developed. Figure 3 depicts the dimensions and boundary conditions of the numerical model.

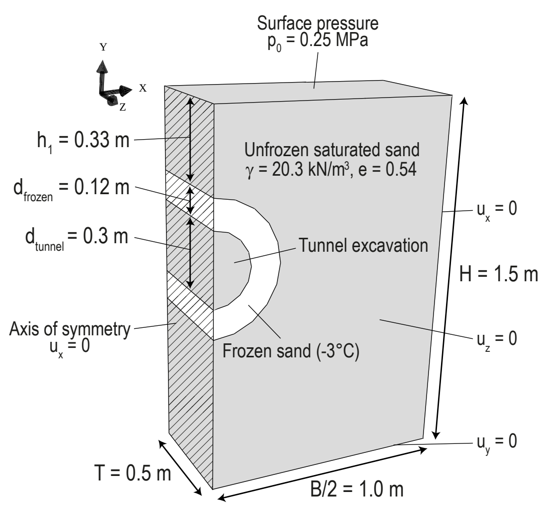

Figure 5. 3D numerical model of a conventional tunnel excavation covered by a frozen soil ring following Orth and Meissner (1985). Figure reproduced from Schindler et al. (2023a).

The numerical simulation consists of the following four steps:

- Geostatic equilibrium step
- Freezing step
- Tunnel excavation step with a step time duration of 13 h
- Creep step with a step time duration of 227 h

For the simulation, we adopted the already calibrated material parameters for frozen Karlsruhe medium sand introduced in Cudmani et al. (2022) and Schindler et al. (2023b), while the unfrozen sand was simulated with a hypoplastic soil model.

Back-calculation of the model test using EVPFROZEN

Figure 6 compares the measured and calculated settlements above the tunnel roof after the tunnel excavation started. As mentioned at the beginning of this section, Orth and Meissner (1985) monitored the displacement/settlement above the tunnel roof at various levels throughout testing. They reported that the settlement at these levels decreased with increasing distance from the tunnel excavation area. In Figure 6, only the largest measured deformations (symbols) are shown, which were consequently monitored close above the tunnel crown near Point A.

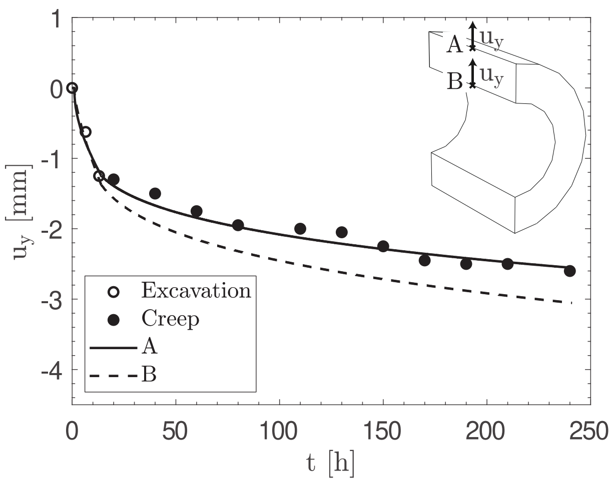

Figure 6. Experimental (symbols) and numerical (solid line) results of the vertical displacement u_y at the tunnel crown centre after beginning the tunnel excavation. [Data from Orth and Meissner (1985)]. Figure reproduced from Schindler et al. (2023a).

The calculated vertical displacements of the two centre points, A and B, at the top and bottom of the frozen tunnel crown are in good agreement with the monitored deformations in the test. As expected, the frozen soil next to the tunnel excavation area (Point B) creeps faster than at the upper part (Point A) due to the higher stress states at the free edge of the frozen soil ring. Consequently, the predicted settlements at Point B are higher than at Point A. In general, the numerical results during the tunnel excavation and the following creep step are qualitatively and quantitatively similar to the measured deformations in the experiments. The tunnel excavation results in a nearly linear increase of the settlements during the excavation time. Afterward, the calculated and measured vertical displacement u_y decrease with increasing creep time. From a practical point of view, the long-analysed creep time of over 200 hrs (more than eight days) represents routine tunnel construction periods (e.g., cross passages) in which the frozen soil body has to bear the loads. Subsequently, the tunnel shot-/concrete support has hardened sufficiently and is able to bear the loads permanently.

This is a post-print of the paper accepted for publication at the 11th International Symposium on Ground Freezing (2023), London (UK).
The final version of the paper, including conference editing/formatting, has been published in the corresponding proceedings:
Schindler, U., Chrisopoulos, S., Cudmani, R. 2023. An advanced constitutive model for AGF design: From calibration to application.
In 11th International Symposium on Ground Freezing. pp. 517-525. London, UK.

CONCLUSIONS

This study deals with the calibration and testing of a novel constitutive model (EVPFROZEN) for frozen granular soils in both small-scale element and large-scale model tests. The unambiguous and rather simple calibration procedure is illustrated by the determination of all eleven model parameters for frozen Manchester fine sand (MFS). The extensive comparison of experimental and numerical uniaxial creep and triaxial compression test results for frozen MFS validates the model response for a wide range of different strain rates, stress states and temperatures. After testing EVPFROZEN in single-element tests, we demonstrated the model's practical effectiveness for AGF design by simulating a tunnel excavation supported by a frozen soil body in order to evaluate the associated deformations during the excavation and creep stages. The predicted incremental displacements above the tunnel crown were in good accordance with the model test data found in the literature. Based on the extensive EVPFROZEN testing and validation with the help of element and model tests, we can enumerate the most important advantages of using EVPFROZEN in AGF designs:

- The EVPFROZEN model only requires a single, relatively small, unambiguously determinable set of material parameters to model a wide range of temperatures, stress states, and strain rates.
- It provides an incremental assessment of the rate-, stress- and time-dependent frozen soil lifetime t_m , i.e. the time at which the frozen soil becomes unstable under constant loading.
- EVPFROZEN can consider the actual temperature distribution within the frozen soil body based on thermal calculations in contrast to a constant average temperature often used in semi-analytical and elastic approaches. Taking into account areas with lower temperatures than the average offers the opportunity to further optimise the AGF design since the shear stiffness, shear strength and frozen soil lifetime increase, while the creep deformations decrease with decreasing temperatures.

REFERENCES

Andersen, G. R. (1991). Physical mechanisms controlling the strength and deformation behaviour of frozen sand (Doctoral dissertation). Massachusetts Institute of Technology.

Cudmani, R., Yan, W., & Schindler, U. (2022). A constitutive model for the simulation of temperature-, stress- and rate-dependent behaviour of frozen granular soils. *Géotechnique*, doi: 10.1680/jgeot.21.00012. Ahead of print.

Martin, R. T., Ting, J. M., & Ladd, C. C. (1981). Creep behaviour of frozen sand (No. R81-19 Final Rpt.). Massachusetts Institute of Technology.

Orth, W. (1986). Gefrorener Sand als Werkstoff: Elementversuche und Materialmodell (Doctoral dissertation). Institut für Bodenmechanik und Felsmechanik der Universität Fridericiana in Karlsruhe. Vol. 100. (in German).

Orth, W. & Meissner, H. (1985). *Experimental and numerical investigations for frozen tunnel shells*. In Fourth International Symposium on Ground Freezing, pages 259–62, Sapporo, Japan.

Schindler, U., Chrisopoulos, S., & Cudmani, R. (2023a). Artificial ground freezing applications using an advanced elastic-viscoplastic model for frozen granular soils. *Cold Regions Science and Technology*. doi: 10.1016/j.coldregions.2023.103964. Ahead of print.

Schindler, U., Cudmani, R., Chrisopoulos, S. & Schünemann, A. (2023b) Multi-stage creep behaviour of frozen granular soils: Experimental evidence and constitutive modelling. *Canadian Geotechnical Journal*. doi: 10.1139/cgj-2022-0637. Ahead of print.

Swan, C. W. (1995). Physical mechanisms controlling the strength and deformation behaviour of unfrozen and frozen Manchester fine sand (Doctoral dissertation). Massachusetts Institute of Technology.

Ting, J. M. M. (1981). The creep of frozen sands: Qualitative and quantitative models (Doctoral dissertation). Massachusetts Institute of Technology.

This is a post-print of the paper accepted for publication at the 11th International Symposium on Ground Freezing (2023), London (UK).
The final version of the paper, including conference editing/formatting, has been published in the corresponding proceedings:
Schindler, U., Chrisopoulos, S., Cudmani, R. 2023. An advanced constitutive model for AGF design: From calibration to application.
In 11th International Symposium on Ground Freezing. pp. 517-525. London, UK.